

Apoptosis and Epicardial Contributions Act as Complementary Factors in Remodeling of the Atrioventricular Canal Myocardium and Atrioventricular Conduction Patterns in the Embryonic Chick Heart

Rebecca Vicente Steijn,¹ David Sedmera ,^{2,3} Nico A. Blom,⁴ Monique Jongbloed,¹ Alena Kvasilova ,² and Ondrej Nanka *^{2*}

¹Department of Anatomy & Embryology, Cardiology, Leiden University Medical Center, Leiden, The Netherlands

²Institute of Anatomy, First Faculty of Medicine, Charles University, Prague, Czech Republic

³Institute of Physiology, Czech Academy of Sciences, Prague, Czech Republic

⁴Department of Pediatric Cardiology, Leiden University Medical Center, Leiden, The Netherlands

Background: During heart development, it has been hypothesized that apoptosis of atrioventricular canal myocardium and replacement by fibrous tissue derived from the epicardium are imperative to develop a mature atrioventricular conduction. To test this, apoptosis was blocked using an established caspase inhibitor and epicardial growth was delayed using the experimental epicardial inhibition model, both in chick embryonic hearts. **Results:** Chicken embryonic hearts were either treated with the peptide caspase inhibitor zVAD-fmk by intrapericardial injection *in ovo* (ED4) or underwent epicardial inhibition (ED2.5). Spontaneously beating embryonic hearts isolated (ED7–ED8) were then stained with voltage-sensitive dye Di-4-ANEPPS and imaged at 0.5–1 kHz. Apoptotic cells were quantified (ED5–ED7) by whole-mount LysoTracker Red and anti-active caspase 3 staining. zVAD-treated hearts showed a significantly increased proportion of immature (base to apex) activation patterns at ED8, including ventricular activation originating from the right atrioventricular junction, a pattern never observed in control hearts. zVAD-treated hearts showed decreased numbers of apoptotic cells in the atrioventricular canal myocardium at ED7. Hearts with delayed epicardial outgrowth showed also increased immature activation patterns at ED7.5 and ED8.5. However, the ventricular activation always originated from the left atrioventricular junction. Histological examination showed no changes in apoptosis rates, but a diminished presence of atrioventricular sulcus tissue compared with controls. **Conclusions:** Apoptosis in the atrioventricular canal myocardium and controlled replacement of this myocardium by epicardially derived HCN4-/Trop1- sulcus tissue are essential determinants of mature ventricular activation pattern. Disruption can lead to persistence of accessory atrioventricular connections, forming a morphological substrate for ventricular pre-excitation. *Developmental Dynamics* 247:1033–1042, 2018. © 2018 Wiley Periodicals, Inc.

Key words: ventricular pre-excitation; chick embryo; optical mapping; atrioventricular junction; apoptosis; epicardial inhibition

Submitted 29 January 2018; First Decision 26 May 2018; Accepted 31 May 2018; Published online 28 August 2018

Introduction

The electrical impulse that triggers the heartbeat is physiologically generated in the sino-atrial node. After rapid spreading through the atrial myocardium, it is delayed in the atrioventricular (AV) node before entering the His-Purkinje system that assures quick and coordinated contraction of the ventricular myocardium.

Grant sponsor: Grant Agency of the Czech Republic; Grant numbers: 13-12412S, 16-02972S; Grant sponsor: Ministry of Education; Grant number: PROGRESS-Q38; Grant sponsor: Charles University SVV, and Academy of Sciences institutional RVO; Grant number: 67985823.

*Correspondence to: Ondrej Nanka, Charles University, First Faculty of Medicine, Institute of Anatomy, U Nemocnice 3, 128 00 Praha 2, Czech Republic. E-mail ondrej.nanka@lf1.cuni.cz

During cardiogenesis, the AV delay appears simultaneously with chamber formation, at embryonic day (ED) 3 in the chick and 9 in the mouse embryo (reviewed in Sedmera et al., 2015). This delay is important for proper ventricular filling by atrial contraction.

Supraventricular tachycardias (SVTs) are the most common type of cardiac arrhythmias in adults and children, with an estimated incidence of 36/100,000 person-years (Lee et al., 2008a). In the majority of cases the mechanism of the SVT involves the presence of an AV myocardial accessory pathway (AP) between the atria and ventricles that serves as substrate for an AV reentry

Article is online at: <http://onlinelibrary.wiley.com/doi/10.1002/dvdy.24642/abstract>
© 2018 Wiley Periodicals, Inc.

tachycardia (AVRT) (Lee et al., 2008a, 2008b). AVRTs represent ~80% of the arrhythmogenic events in both the fetus and the newborn and ~30% of SVTs in adults. In infants with a structurally normal heart, the first episode of AVRT tends to occur before birth or within the first months of life and usually resolves spontaneously before the age of 1 year. However, if AVRT is diagnosed later in life, spontaneous resolution only occurs in 15% of the cases (Lee et al., 2008b).

The presence of an AP can lead to premature activation of the ventricles and predispose to AVRT due to anterograde (atrium-to-ventricle) AP conduction as seen in the Wolff-Parkinson-White (WPW) syndrome. APs are anatomically widely distributed and have been identified throughout the entire annulus fibrosus at both the mitral and tricuspid annulus and septal region. *Right-sided* pathways are more commonly found in neonates and young patients whereas in adults with WPW syndrome APs are more often located at the *left* annulus (Ko et al., 1992).

The exact origin and electrophysiological properties of APs underlying AVRT is presently unknown. Understanding the embryological mechanisms that can lead to AP formation would, therefore, be important. The annulus fibrosus and the AV myocardium are two indispensable structures within the heart for normal development of the AV junction (Wessels et al., 1991).

During early development, the heart starts off as a linear tube formed by an endocardial and a myocardial layer (Jongbloed et al., 2012). The embryonic AV canal myocardium is a circumferentially aligned myocardial funnel between the atria and ventricles, initially situated above the primitive left ventricle. Like other slowly conducting areas of the heart, the AV canal myocardium shows a specific expression profile resembling that of the primitive heart tube and cardiac conduction system (Aanhaanen et al., 2011; Vicente-Steijn et al., 2011). During cardiogenesis, the heart receives additional cells that reside outside the heart (reviewed in Buckingham et al., 2005; Jongbloed et al., 2012). One of these cell populations originates from the proepicardial organ (PEO), a transient cluster of cells located in the sinus venosus (inflow) segment of the heart (Gittenberger-de Groot et al., 1998,2012). Epicardial cells that will form the epicardial layer of the heart originate from the PEO. After spreading over the heart, a subset of cells will undergo epithelial-to-mesenchymal transition, form the subepicardial layer and become epicardium-derived cells (EPDCs).

Subsequently, a subset of EPDCs with a gene expression profile distinct from ventricular EPDCs (Zhou et al., 2010) will form the annulus fibrosus (Lockhart et al., 2014). The annulus subset of EPDCs will invade the lower AV canal myocardium area, pushing the AV canal myocardium into the atrial chambers (Wessels et al., 1991). During human fetal life many APs originate from this region (Hahurij et al., 2008), which, in the embryonic chicken, still show a cardiac conduction system expression profile (Kolditz et al., 2008; Vicente-Steijn et al., 2011).

After normal formation of the annulus fibrosus, the AV conduction axis (i.e., the AV node and the bundle of His) will eventually remain as the only myocardial connection between the atria and ventricles, ensuring proper propagation of the electrical impulse (Jongbloed et al., 2012). Abnormal development of the annulus fibrosus in animal models results in persistent myocardial AV continuities and ultimately in ventricular pre-excitation (Gaussin et al., 2005; Kolditz et al., 2008). Defective AV canal myocardium development triggered by mutations in Notch signaling (Rentschler et al., 2011) and *Tbr2* (Aanhaanen et al.,

2011) results in AP formation and ventricular pre-excitation in the mouse. Conversely, complete interruption of the AV conduction axis in pregnancies complicated by presence of maternal anti-lupus antibodies can result in complete AV block, a serious fetal complication with high morbidity and mortality and unclear treatment options (reviewed in Sedmera et al., 2015).

Apoptosis plays an important part of the AV myocardium remodeling (Cheng et al., 2002), occurring at the time of maturation of the ventricular conduction patterns (Reckova et al., 2003). This results in an apex to base activation of the ventricles, as opposed to an immature base to apex activation at earlier stages (Reckova et al., 2003). Increased apoptosis was observed in the AV myocardium of quail embryos incubated in hypoxia. These hearts showed precocious appearance of mature apex to base ventricular activation patterns (Nanka et al., 2008), suggesting that programmed cell death plays an important role in pruning the AV conduction axis, as it does in proper outflow tract septation (Sugishita et al., 2004).

Based upon these studies, we hypothesized that the two important mechanisms involved in the myocardial pruning of the AV conduction pathway, i.e., apoptosis and epicardial invasion, ensure that the AV node and His bundle remain the only myocardial connection that propagates the electrical impulse from atria to ventricles. In the present study, we have studied both processes throughout chicken heart development to elucidate their role in formation of APs and ventricular pre-excitation. We found that inhibition of apoptosis led to persistence of immature activation patterns including abnormal activation from the right AV junction. Epicardial inhibition likewise led to immature ventricular activation, but the activation originated from the left side and apoptosis rates were not altered. Together, we consider these two cellular mechanisms as a complementary physiological way of remodeling the AV myocardium.

Results

Normal Development

Normal development of the AV junction was characterized by a gradual transformation of the AV canal myocardium into HCN4-/Trop1- sulcus tissue (annulus fibrosus development), with the AV bundle forming eventually the only myocardial continuity between the atrial and ventricular myocardium (Fig. 1). 3D reconstructions performed between ED4 and ED8 showed the position and extent of the HCN4 positive AV myocardium in relation to the annulus fibrosus development. At Hamburger and Hamilton stage (HH) 24 (ED4), we could observe the primitive state of AV canal myocardium as a continuous conduction path between the atria and ventricles with no isolation between them. In contrast, reconstruction at HH 33 (ED8) showed the more mature state of the AV myocardium where it is mainly located at the atrial level and isolated from the ventricles by the investing annulus fibrosus (Fig. 2).

During the course of development between ED4 and ED8, we observed a gradual increase in frequency of the mature apex-to-base activation patterns, in agreement with previous studies (Reckova et al., 2003; Sedmera et al., 2008). The epicardial ventricular activation time increased with development, together with ventricular enlargement. As maturation of the activation patterns of the heart proceeded, the ventricular activation times decreased. There were significant differences in activation times

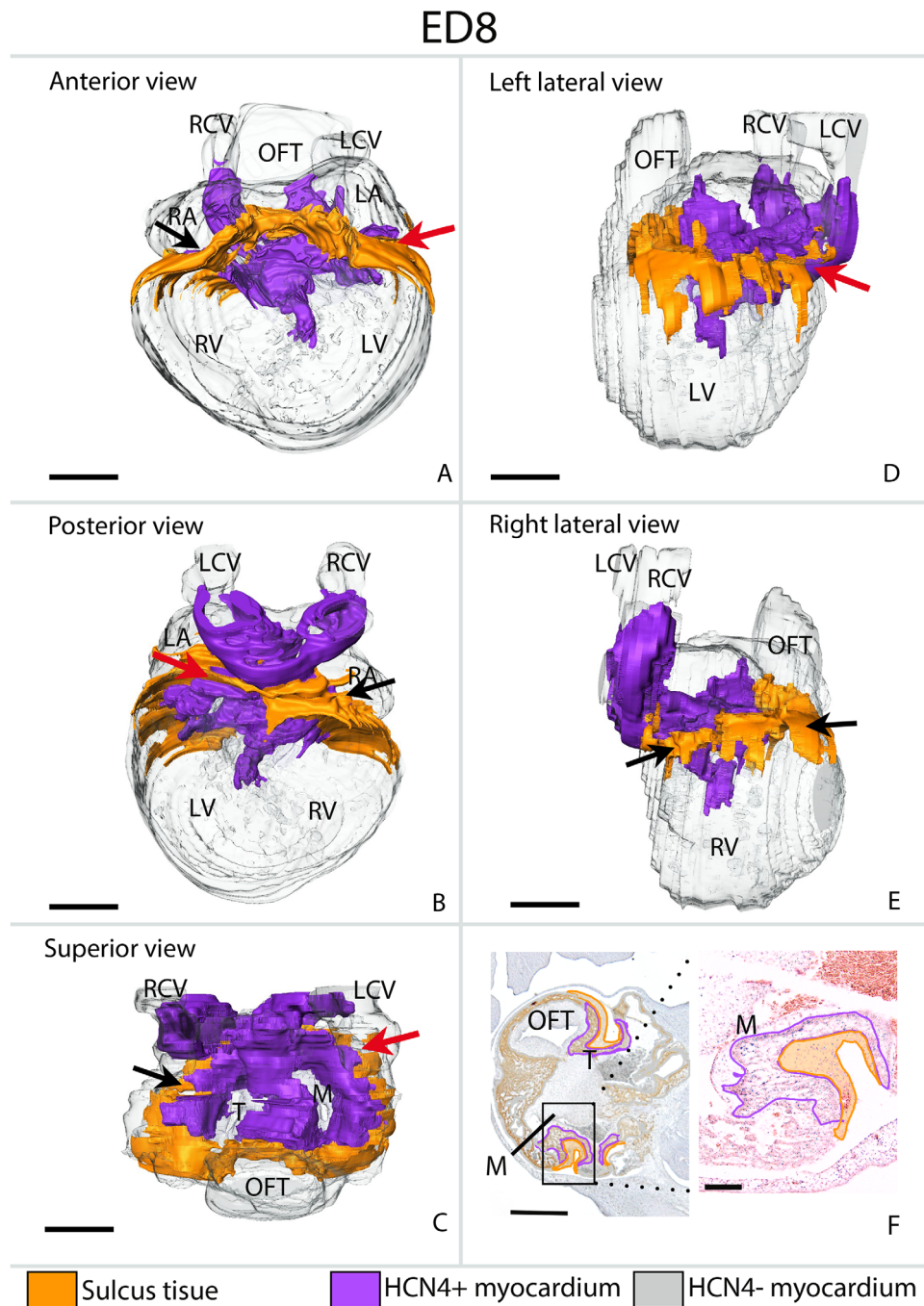


Fig. 2. Development of the AV junction in the chick (ED8). **A–E:** 3D reconstructions of chick hearts at developmental stage ED8 (approx. HH33), shown from different angles as indicated. Color coding is as in Figure 1. HCN4 negative atrial and ventricular myocardium and lumen of the cardinal veins have been rendered transparent. Sulcus tissue is now present at the left AV junction, however, progression is still less than at the right AV junction (compare lack and red arrows in B) and less at the left posterior wall as compared to the right side (compare black and red arrows in C, also see red arrow in D). **F:** Histological sections at the level of the AV canal (AVC) stained with cardiac troponin I (cTropI, left side) and HCN4 (right side). In the troponin stained section (left), annotation used to develop the 3D reconstructions is shown by the orange and purple lines to show sulcus tissue and HCN4 positive AV myocardium, respectively. A, atria; AVC, atrioventricular canal; LA, left atrium; LCV, left cardinal vein; LV, left ventricle; OFT, outflow tract; RA, right atrium; RCV, right cardinal vein; RV, right ventricle; V, ventricle.

patterns, some of which originated from the right AV junction (Fig. 3, right panel). This was preceded by observation of a significant reduction of apoptotic cells in the entire AV myocardium at ED6 (7 ± 1 vs. 15 ± 2 , $n = 6$, detected by Lysotracker Red), confirmed by whole-mount caspase immunostaining at ED7 (Fig. 4). However, at an earlier time point (ED5, 24 hr

after application), there were no differences between groups, excluding significant cytotoxicity of the compound or the application mode (data not shown). The outflow tract at ED8 was elongated and pulsatile, serving as a validation of phenotype of inhibition of myocardial apoptosis (Watanabe et al., 2001).

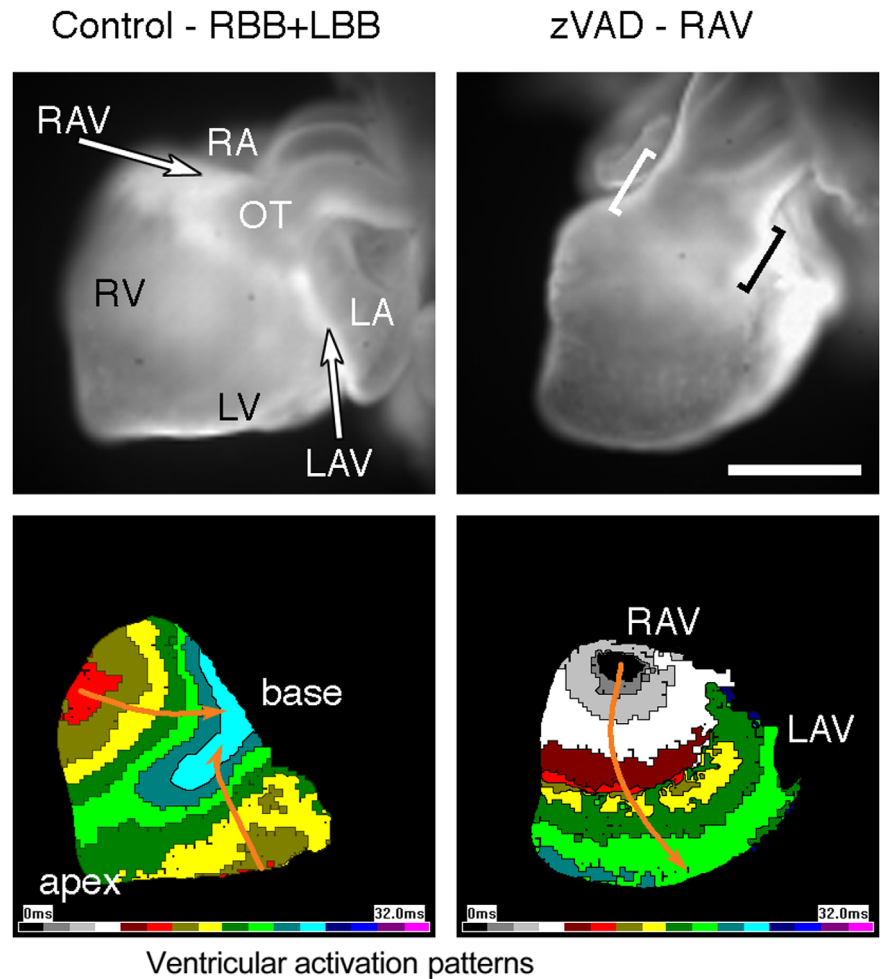
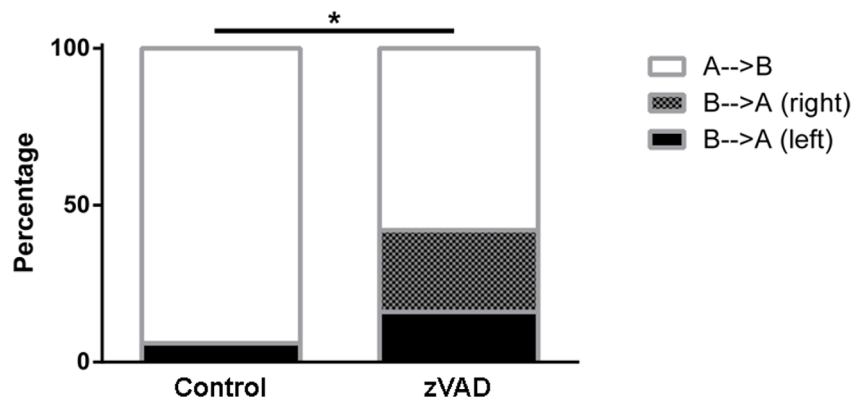


Fig. 3. Effect of apoptosis inhibition on ventricular activation patterns. In zVAD-treated hearts, abnormal activation originating from right AV junction (orange arrows) was observed at ED8. There was a significant increase in the proportion of immature (base-to-apex) patterns in this group. $N = 13$ and 26 , $*P < 0.05$ by χ^2 test; scale bar $500 \mu\text{m}$. A, apex; B, base; LA, left atrium; LAV, left atrioventricular junction; LV, left ventricle; OT, outflow tract; RA, right atrium; RAV, right atrioventricular junction; RV, right ventricle.



In most cases, the immature activation originated from the right atrioventricular junction, which was not observed in the control hearts (Fig. 3). This correlated well with approximately 50% decreased apoptosis in the AV canal 1 day before mapping, present on both sides but more significant in the right AV junction (Fig. 4).

Epicardial Inhibition

To investigate the cellular changes in a previously established model of epicardial ablation that leads to persistence of myocardial atrioventricular connections (Kolditz et al., 2008), we performed optical

mapping and histological studies at various stages after epicardial inhibition. There were no significant differences or abnormal activation patterns observed at ED3.5–ED5.5. At both ED7.5 and ED8.5, we observed a significantly increased proportion of immature activation patterns in the epicardially inhibited hearts (Fig. 5). In cases presenting persisting immature base-to-apex activation patterns, the ventricles were always activated from the left AV junction.

Histological analysis confirmed the abnormal epicardial covering with persisting myocardial atrioventricular continuity but showed no changes in apoptosis rates by anti-active caspase-3 immunohistochemistry (Fig. 6, and data not shown).

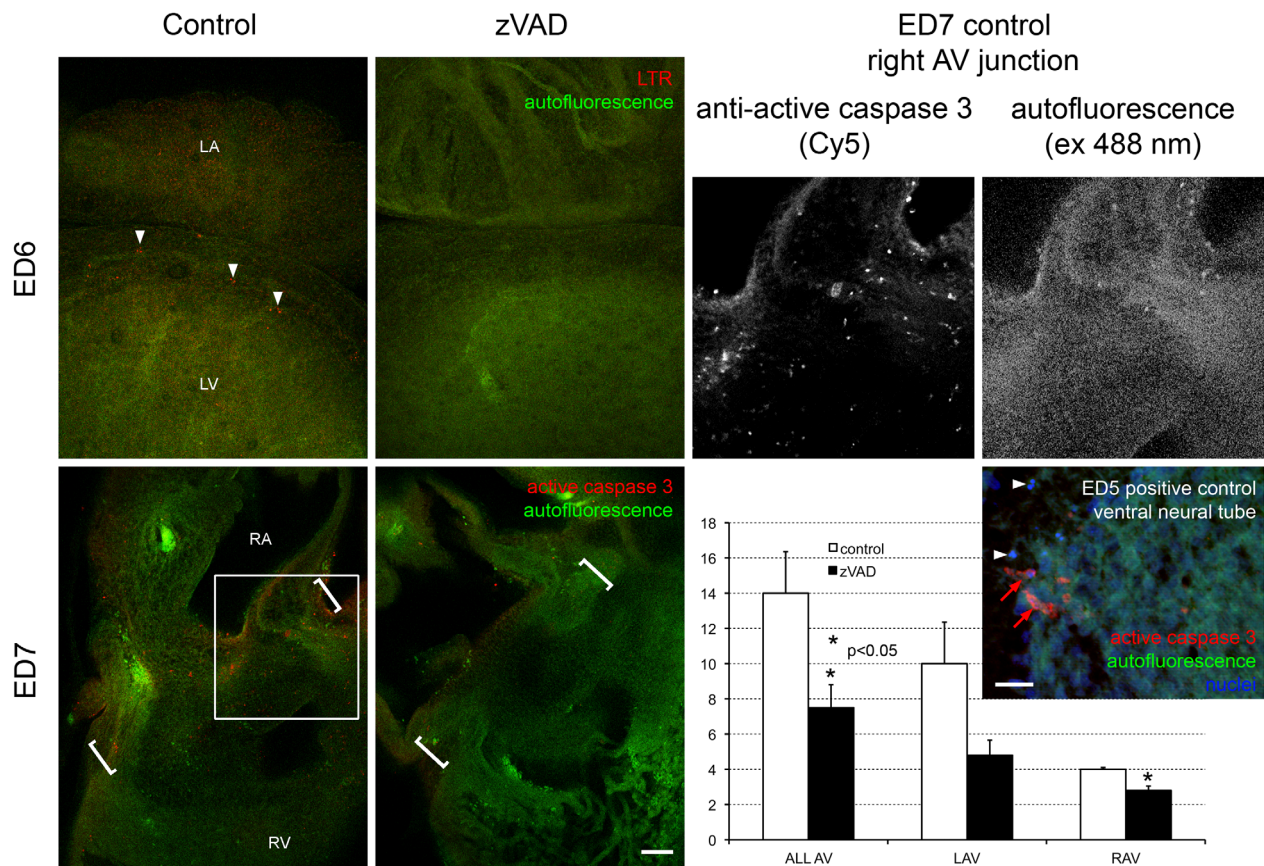


Fig. 4. zVAD treatment decreased the number of apoptotic cells in the AV canal myocardium. Decrease was evident on both ED6 and ED7 and was present in both left and right portion of the AV canal. Grayscale panels show independently the red (signal) and green (autofluorescence) channels from the boxed area. Positive control (red arrows) shows high magnification view of ventral neural tube at ED5 from sections analyzed in the epicardially inhibited embryos. Apoptotic bodies (final stage) are indicated by white arrowheads. Values are mean \pm SEM, N = 6, * P < 0.05 by t -test. Scale bar = 100 μ m, 10 μ m for the positive control.

Discussion

During normal chick heart development, maturation of the ventricular activation pattern is observed around the time of ventricular septation (Chuck et al., 1997; Reckova et al., 2003). In our previous studies (Reckova et al., 2003; Hall et al., 2004; Sedmera et al., 2008), we have focused mainly on the effects of various experimental manipulations on the differentiation of the fast-conducting component (i.e., formation of the His-Purkinje network from the ventricular trabeculae). However, other studies (Gurjarpadhye et al., 2007; Kolditz et al., 2008) have pointed out that ventricular activation pattern is equally dependent on the nature of the AV connections, and possibly the fibrous insulation between the AV and ventricular myocardium. In agreement with quantification of duration of epicardial ventricular activation ("pseudo-QRS") performed in the mouse (Sankova et al., 2012), we have observed that mature apex to base activation patterns were always faster than the immature base to apex activation patterns at the same stage.

Based on our findings that hypoxia seemed to accelerate maturation of the ventricular activation sequence through increased apoptosis in the AV myocardium (Nanka et al., 2008), we performed inhibition experiments using zVAD-FMK peptide according to the previously established model of Watanabe et al. (2001), which lead to persistence of the outflow tract

myocardium (Fig. 3, top right panel), normally almost completely eliminated largely through apoptosis (Pexieder, 1972, 1973). At ED8, when the majority of normal hearts shows mature ventricular activation from the ventricular apices, the zVAD-treated hearts showed activation from the ventricular base, suggestive of persisting atrioventricular continuity. Of note, in most cases, the activation originated from the right atrioventricular junction, only extremely rarely observed during normal development before ED7/HH stage 31. This correlated well with the decreased apoptosis in the AV canal 1 day before mapping, present on both sides but more significant in the right AV junction.

As such disappearance of myocardium needs to be replaced by another tissue to maintain heart wall integrity, we studied also the development of fibrous insulation by HCN4-/Trop1- sulcus tissue originating from the epicardium. This logically resulted in use of an experimental perturbation model of annulus fibrosus formation (Kolditz et al., 2008) as a second mechanism. While there were no significant differences in activation patterns at the early stages where the myocardial AV continuity is normally still unbroken, from ED7.5 onward, there was a significantly increased proportion of persisting immature activation patterns suggesting abnormal myocardial continuity. In hearts with histologically confirmed epicardial ablation, we noted abnormal activation patterns of the ventricles similar to those observed

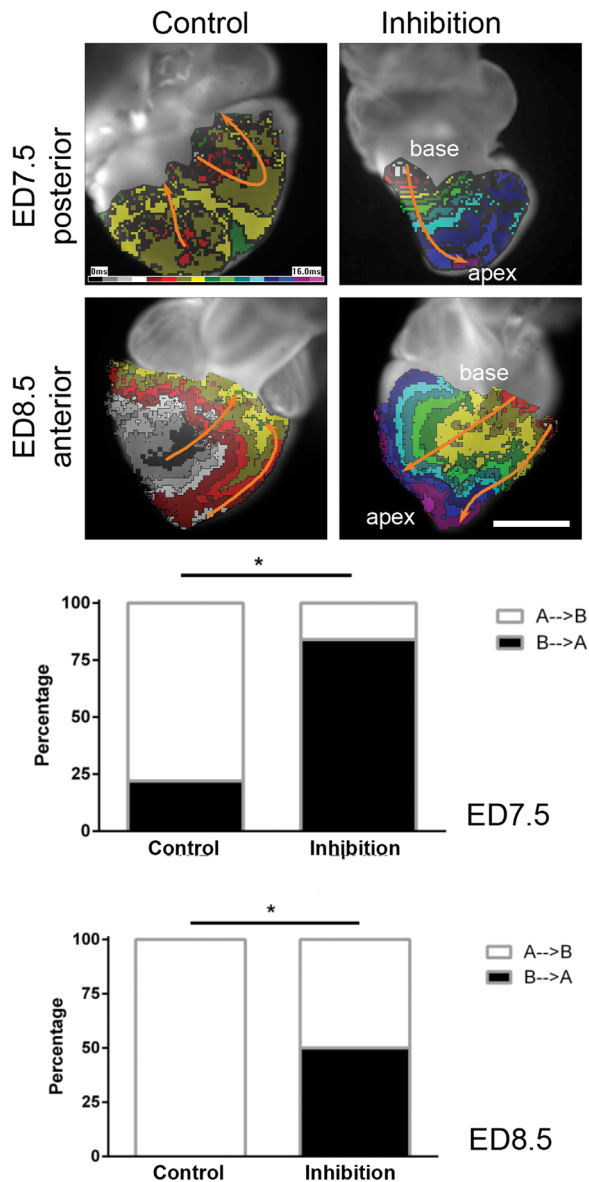


Fig. 5. Epicardial inhibition results in persistence of immature activation patterns. Percentage of immature (base-to-apex) patterns was significantly increased in the inhibited group at both ED7.5 and 8.5. Typical examples of maps showing the immature patterns are shown in the upper panels together with controls, showing apex-to-base activation from 2 centers (left and right). $N = 8$ and 9 (ED7.5), 11 and 8 (ED8.5), $*P < 0.05$ by χ^2 test. Scale bar = $500 \mu\text{m}$. Orange arrows indicate the direction of activation. The color bar of isochrones (1-ms intervals) in the top left panel is valid also for the other ones.

after apoptosis blockade. However, in cases of persisting immature base-to-apex activation, the ventricles were always activated from the left AV junction. The process of epicardial invasion seems to operate independent of apoptosis, because no significant changes in the numbers of dying cells were observed in the ablated hearts.

Right-sided pathways are more commonly found in neonates and young patients whereas in adults with WPW syndrome APs are more often located at the left annulus (Ko et al., 1992). Based on our findings, it is tempting to speculate that this relates to different, complementary, mechanisms involved in pruning of

the AVC junction. An imbalance in the amount of programmed cell death, e.g., due to hypoxia, may contribute to occurrence of right-sided APs, whereas deficient epicardial contribution may relate to APs in the left AV junction that may expose themselves functionally later in life.

Conclusion

We provide experimental evidence supporting programmed cell death and epicardial invasion as two independent mechanisms reducing the originally broad myocardial AV continuity of poikilotherms and young embryos to a single pathway consisting of the AV node and His bundle characteristic of fetal and adult homeotherms. This pruning of the AV conduction pathway was hypothesized to be necessary to sustain the high heart rates of birds and mammals (Davies et al., 1952) and indeed might be protective against AV reentry (Sedmera et al., 2015). Further experiments could test the potential of the respective cell populations *in vitro*, where further manipulations are possible and the nature of signaling or tissue interactions could be dissected more precisely.

Study Limitation

Cardiac nonmyocytes are currently regarded as a mosaic originating from several sources (endothelial-mesenchymal transformation, epicardium, blood stream origin, neural crest), so we cannot exclude significant contribution to annulus fibrosus from these other sources, which can compensate later in development as a potential backup mechanism. Similarly, the surviving AV myocytes could still die later in development (e.g., during the early postnatal period characterized by a wave of apoptosis, Kajstura et al., 1995), resulting in disappearance of these abnormal connections. The widely applied method to achieve impaired epicardial development was applied. This resulted in a delay in epicardial covering of the heart, not in a complete lack of epicardial development. Thus, an epicardial covering of the heart was observed at the late stages of development but was different from control hearts. Apical parts of the ventricles still showed lack of epicardial covering and the thickness of the subepicardial layer was smaller than in controls.

Experimental Procedures

Animal Preparation

Animal experiments were performed in accordance to institutional guidelines of the Leiden University Medical Center and in compliance with guidelines from Directive 2010/63/EU of the European Parliament on the protection of animals used for scientific purposes. The embryonic surgery and chemical treatment of chicken eggs is exempt according to the Czech law. Fertilized White Leghorn chicken eggs were incubated blunt end up at 37.5°C and 50% humidity with periodic turning. Embryos were staged according to the HH criteria (Hamburger and Hamilton, 1951).

Inhibition of Apoptosis

Inhibition of apoptosis was accomplished by intra-pericardial injection of zVAD-FMK (Watanabe et al., 2001). The eggs incubated for 4 days (to HH stage 24) were windowed on the blunt

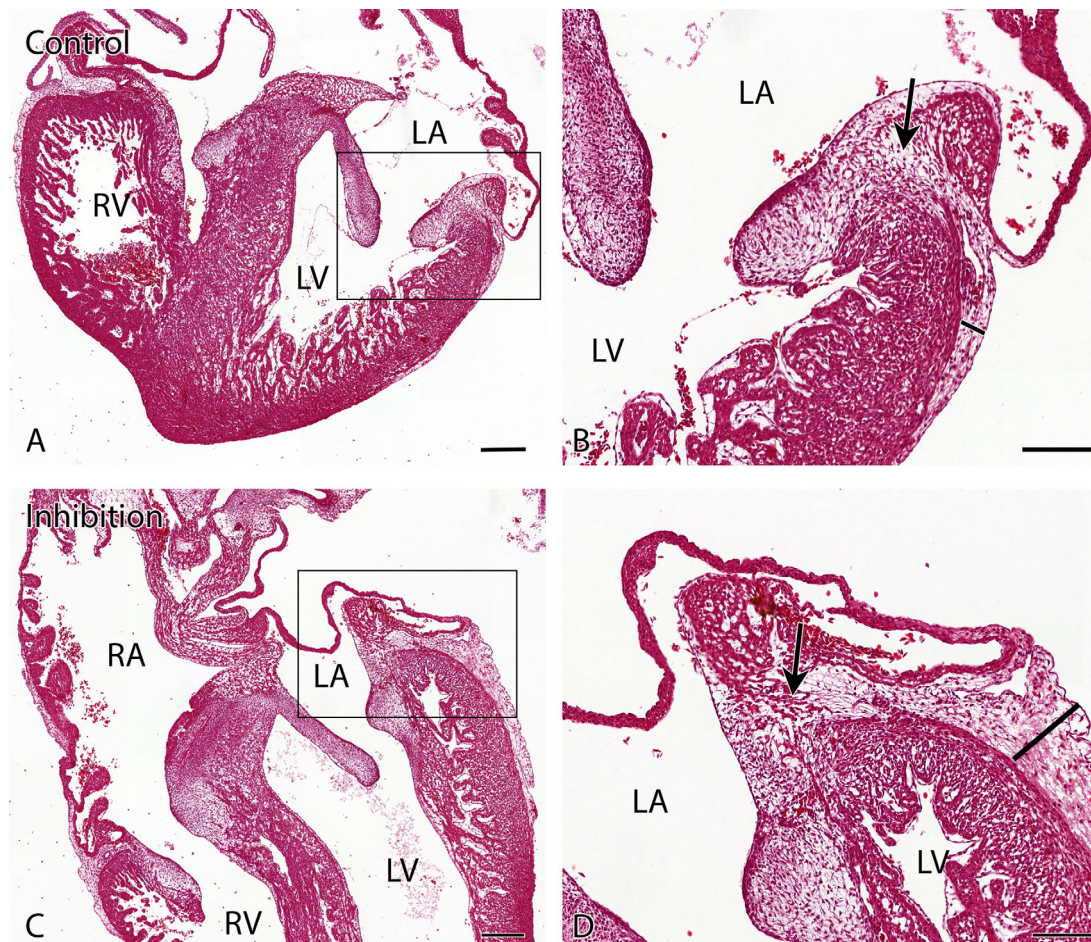


Fig. 6. A–D: Histology of control and epicardially inhibited hearts at ED8.5. Note the increase thickness of the epicardium (lines) and persistence of the left atrioventricular continuity (arrows) in the experimental heart. Haematoxylin and eosin staining. Scale bars = 200 μ m in A,C; 100 μ m in B,D.

end, and the embryos were exposed by partial removal of the inner shell membrane and opening of the amniotic cavity. Under microscopic control, 1 μ l of dimethyl sulfoxide (DMSO) containing 1 mg/25 μ l of zVAD-fmk (Calbiochem) was injected into the pericardial cavity using a pulled glass needle, as described (Watanabe et al., 2001). Controls received 1 μ l of DMSO. Despite temporary heart arrest, the survival was identical for both the solvent and zVAD group (77%, N = 13 and 26, respectively). Sampling for optical mapping was performed at ED8, by which time most hearts should show mature ventricular activation pattern (Reckova et al., 2003). Sampling for histology was performed at ED5, ED6, and ED7 (N = 6 per stage), when apoptosis in the AV canal is the most abundant (Cheng et al., 2002).

Epicardial Inhibition

Partial-to-complete inhibition of outgrowth of the proepicardial organ (PEO) was accomplished by in ovo micromanipulation in a similar way as first described by Manner (Manner, 1993) and performed previously in our lab (Kolditz et al., 2008). Briefly, to prevent the epicardial covering of the heart, a piece of eggshell membrane was positioned between the PEO and the heart on ED2.5 (HH15–HH16). After placement of the membrane, the eggs were resealed and re-incubated until the embryos reached the desired developmental stage. Sampling for optical mapping followed by

histological examination (to confirm ablation phenotype) was performed daily from ED3.5 until ED8.5 (N \geq 8 per stage) (Fig. 6).

Whole-Mount and Tissue Sections for Nonradioactive In Situ Hybridization for HCN4

Whole-mount in situ hybridization (ISH) was performed according to published protocol (Nieto et al., 1992). An Hcn4 cDNA template was generated using chicken Hcn4-specific primers (forward: 5'-GTGTCAGTGGGATGGCTGCCT-3', reverse: 5'-CCAA TGGTGCCTCCCGAA-3'). These primers produced a purified cDNA fragment corresponding to amino acids 400–602 of the chicken predicted Hcn4 sequence (XM_425050 as previously described; Vicente-Steijn et al., 2011). ISH on 10- μ m transversal sections from chicken embryos day E4 and E8 was performed as described previously (Vicente-Steijn et al., 2010). Five embryos per probe (sense/antisense) were used for the whole-mount ISH.

Immunohistochemistry

Immunohistochemical staining was conducted as described previously (Mahtab et al., 2009) on sister sections from the Hcn4 ISH-stained sections (HH15–HH35). The staining was conducted using the primary antibody cardiac troponin I (cTnI, goat polyclonal antibody, sc-15368, Santa Cruz, CA, 1/400. Slides were

incubated with a biotin-conjugated secondary antibody (horse-goat [BA-9500], Vector Labs, Burlingame, CA), visualized by incubation with 3-3'-diaminobenzidine tetrahydrochloride (DAB, D5637, Sigma-Aldrich, St Louis, MO), and counterstained with hematoxylin (0.1%, Merck, Darmstadt, Germany).

Histological Staining

Control and epicardial inhibition hearts (ED 8, HH33/HH34) were fixed in 4% paraformaldehyde for 24 hr, embedded in paraffin and serially sectioned (5- μ m sections). Histochemical stainings were performed with hematoxylin-eosin (HE) staining (hematoxylin: KlinePath; eosin: Tissue-Tek/Sakura) as previously described (Kelder et al., 2015). Briefly, after rehydration, sections were stained for hematoxylin for 5 min after which the sections were rinsed 10 min in tap water. After briefly rinsing in milliQ water, counterstaining with eosin was performed for 1 min. Finally, the sections were rinsed with tap water for 10 min, dehydrated, and mounted in Entellan (Merck).

3D Reconstructions

3D reconstructions of atrial and ventricular myocardium of TNNI2-stained serial sections of HH24 and HH33 embryos were made as previously described (Vicente-Steijn et al., 2011) using the AMIRA v5.0 Software Package (Template Graphics Software, San Diego, CA). The *HCN4* positive myocardium observed in immediate sister sections was superimposed.

Functional Recordings

Optical mapping recordings were conducted as previously described (Sankova et al., 2010). Briefly, freshly isolated hearts from ED4-ED8.5 (HH24-HH35) chick embryos were dissected in ice-cold (to reduce any hypoxic damage) Tyrode's solution with the following composition: NaCl 145 mmol/l, KCl 5.9 mmol/l, CaCl₂ 1.1 mmol/l, MgCl₂ 1.2 mmol/l, glucose 11 mmol/l, HEPES 5 mmol/l; pH = 7.4. Hearts were isolated with abundant noncardiac outflow tract tissue to allow pinning in the tissue bath and intact inflow tract region to ensure spontaneous beating activity. The hearts were stained with 2.5 mmol/l di-4-ANEPPS (Invitrogen, Carlsbad, CA) for 10 min. Motion control was accomplished with 0.1 μ M blebbistatin (Sigma, Germany) and by pinning the heart by the extracardiac tissue to the bottom of the dish. The Ultima L high-speed camera (SciMedia Ltd., Tokyo, Japan) and bundled software were used for the data acquisition (0.5-1 kHz) and analysis was performed using the BV_Analyzer software bundle as recently described (Sankova et al., 2010). Total ventricular activation time and first ventricular activation site were calculated.

Whole-Mount Cell Death Staining

After isolation from control and treated embryos at ED5, ED6, and ED7, the hearts were whole-mount stained with 0.1 μ M LysoTracker Red in Tyrode's (Molecular Probes, now Thermo Fisher Scientific, Inc.) for 1 hr as described (Schaefer et al., 2004). After thorough rinsing in Tyrode's, the hearts were fixed in 4% paraformaldehyde in phosphate buffered saline (PBS) at 4°C overnight. After rinsing in PBS, the hearts were microdissected in a transverse plane to provide an unobstructed superior view of the AV region. The slices were dehydrated in ascending

ethanol series and pinned to the bottom of a silicone chamber (Miller et al., 2005). The samples were then cleared in benzyl alcohol:benzyl benzoate mix (50/50) and imaged on an upright Olympus confocal microscope using 4 \times (overview) and 10 \times (detailed series at 3 μ m steps of the left and right AV region).

To confirm the specificity of the LysoTracker Red staining, active caspase 3 (BD Pharmingen, San Diego, CA, clone #C92-605) whole-mount immunohistochemistry was performed. Primary antibody was diluted 1:500, and for detection, goat-anti-rabbit Cy5-coupled secondary antibody (Jackson ImmunoResearch, West Grove, PA, 1:200) was used. The nuclei were counterstained with Hoechst 33342 (Sigma, Germany). Analysis was performed after dehydration and tissue clearing on confocal microscope as described above. No normalization was used, as we counted all the positive cells across the entire AV junction.

Statistical Analysis

Data was analyzed using GraphPad Prism software (GraphPad Software, La Jolla, CA). Results are shown as mean \pm SEM. Differences between groups were analyzed with the independent sample *t*-test when the data showed a normal distribution and with the nonparametric Mann-Whitney *U*-test when the distribution was not normal; *P* < 0.05 was considered to be statistically significant. For comparison of the activation patterns (categorical variable) χ^2 -test was performed. A *P*-value < 0.05 was considered significant.

Acknowledgments

We thank Ms. Marie Jindrakova for her excellent technical assistance, and we greatly acknowledge Bert Wisse for his help with the creation of Figures 1 and 5. This work was supported by the Ministry of Education PROGRESS-Q38, Charles University SVV, and Academy of Sciences institutional RVO: 67985823. D.S. was funded by the Grant Agency of the Czech Republic, and R.V.S. and M.R.M.J. were funded by the Netherlands Heart Foundation. **Conflicts of interest:** None to declare.

References

- Aanhaanen WT, Boukens BJ, Sizarov A, Wakker V, de Gier-de Vries C, van Ginneken AC, Moorman AF, Coronel R, Christoffels VM. 2011. Defective Tbx2-dependent patterning of the atrioventricular canal myocardium causes accessory pathway formation in mice. *J Clin Invest* 121:534-544.
- Buckingham M, Meilhac S, Zaffran S. 2005. Building the mammalian heart from two sources of myocardial cells. *Nat Rev Genet* 6: 826-835.
- Cheng G, Wessels A, Gourdie RG, Thompson RP. 2002. Spatiotemporal distribution of apoptosis in embryonic chicken heart. *Dev Dyn* 223:119-133.
- Chuck ET, Freeman DM, Watanabe M, Rosenbaum DS. 1997. Changing activation sequence in the embryonic chick heart. Implications for the development of the His-Purkinje system. *Circ Res* 81:470-476.
- Davies F, Francis ET, King TS. 1952. The conducting (connecting) system of the crocodilian heart. *J Anat* 86:152-161.
- Gaussin V, Morley GE, Cox L, Zwijsen A, Vance KM, Emile L, Tian Y, Liu J, Hong C, Myers D, Conway SJ, Depre C, Mishina Y, Behringer RR, Hanks MC, Schneider MD, Huylebroeck D, Fishman GI, Burch JB, Vatner SF. 2005. Alk3/Bmpr1a receptor is required for development of the atrioventricular canal into valves and annulus fibrosus. *Circ Res* 97:219-226.

- Gittenberger-de Groot AC, Vrancken Peeters MP, Mentink MM, Gourdie RG, Poelmann RE. 1998. Epicardium-derived cells contribute a novel population to the myocardial wall and the atrioventricular cushions. *Circ Res* 82:1043–1052.
- Gittenberger-de Groot AC, Winter EM, Bartelings MM, Goumans MJ, DeRuiter MC, Poelmann RE. 2012. The arterial and cardiac epicardium in development, disease and repair. *Differentiation* 84:41–53.
- Gurjarpadhye A, Hewett KW, Justus C, Wen X, Stadt H, Kirby ML, Sedmera D, Gourdie RG. 2007. Cardiac neural crest ablation inhibits compaction and electrical function of conduction system bundles. *Am J Physiol Heart Circ Physiol* 292:H1291–H1300.
- Hahurij ND, Gittenberger-De Groot AC, Kolditz DP, Bokenkamp R, Schaliij MJ, Poelmann RE, Blom NA. 2008. Accessory atrioventricular myocardial connections in the developing human heart: relevance for perinatal supraventricular tachycardias. *Circulation* 117:2850–2858.
- Hall CE, Hurtado R, Hewett KW, Shulimovich M, Poma CP, Reckova M, Justus C, Pennisi DJ, Tobita K, Sedmera D, Gourdie RG, Mikawa T. 2004. Hemodynamic-dependent patterning of endothelin converting enzyme 1 expression and differentiation of impulse-conducting Purkinje fibers in the embryonic heart. *Development* 131:581–592.
- Hamburger V, Hamilton HL. 1951. A series of normal stages in the development of the chick embryo. *J Morphol* 88:49–92.
- Jongbloed MR, Vicente Steijn R, Hahurij ND, Kelder TP, Schaliij MJ, Gittenberger-de Groot AC, Blom NA. 2012. Normal and abnormal development of the cardiac conduction system; implications for conduction and rhythm disorders in the child and adult. *Differentiation* 84:131–148.
- Kajstura J, Mansukhani M, Cheng W, Reiss K, Krajewski S, Reed JC, Quaini F, Sonnenblick EH, Anversa P. 1995. Programmed cell death and expression of the protooncogene bcl-2 in myocytes during postnatal maturation of the heart. *Exp Cell Res* 219:110–121.
- Kelder TP, Duim SN, Vicente-Steijn R, Vegh AM, Kruithof BP, Smits AM, van Bavel TC, Bax NA, Schaliij MJ, Gittenberger-de Groot AC, DeRuiter MC, Goumans MJ, Jongbloed MR. 2015. The epicardium as modulator of the cardiac autonomic response during early development. *J Mol Cell Cardiol* 89:251–259.
- Ko JK, Deal BJ, Strasburger JF, Benson DW Jr. 1992. Supraventricular tachycardia mechanisms and their age distribution in pediatric patients. *Am J Cardiol* 69:1028–1032.
- Kolditz DP, Wijffels MC, Blom NA, van der Laarse A, Hahurij ND, Lie-Venema H, Markwald RR, Poelmann RE, Schaliij MJ, Gittenberger-de Groot AC. 2008. Epicardium-derived cells in development of annulus fibrosis and persistence of accessory pathways. *Circulation* 117:1508–1517.
- Lee KW, Badhwar N, Scheinman MM. 2008a. Supraventricular tachycardia—part I. *Curr Probl Cardiol* 33:467–546.
- Lee KW, Badhwar N, Scheinman MM. 2008b. Supraventricular tachycardia—part II. History, presentation, mechanism, and treatment. *Curr Probl Cardiol* 33:557–622.
- Lockhart MM, Phelps AL, van den Hoff MJ, Wessels A. 2014. The epicardium and the development of the atrioventricular junction in the murine heart. *J Dev Biol* 2:1–17.
- Mahtab EA, Vicente-Steijn R, Hahurij ND, Jongbloed MR, Wisse LJ, DeRuiter MC, Uhrin P, Zaujec J, Binder BR, Schaliij MJ, Poelmann RE, Gittenberger-de Groot AC. 2009. Podoplanin deficient mice show a RhoA-related hypoplasia of the sinus venosus myocardium including the sinoatrial node. *Dev Dyn* 238:183–193.
- Manner J. 1993. Experimental study on the formation of the epicardium in chick embryos. *Anat Embryol (Berl)* 187:281–289.
- Miller CE, Thompson RP, Bigelow MR, Gittinger G, Trusk TC, Sedmera D. 2005. Confocal imaging of the embryonic heart: how deep? *Microsc Microanal* 11:216–223.
- Nanka O, Krizova P, Fikrlé M, Tuma M, Blaha M, Grim M, Sedmera D. 2008. Abnormal myocardial and coronary vasculature development in experimental hypoxia. *Anat Rec (Hoboken)* 291:1187–1199.
- Nieto MA, Bennett MF, Sargent MG, Wilkinson DG. 1992. Cloning and developmental expression of *Sna*, a murine homologue of the *Drosophila* snail gene. *Development* 116:227–237.
- Pexieder T. 1972. The tissue dynamics of heart morphogenesis. I. The phenomena of cell death. B. Topography. *Z Anat Entwicklungsgesch* 138:241–253.
- Pexieder T. 1973. The tissue dynamic of heart morphogenesis. II. Quantitative examinations. B. Cell death foci. *Ann d'Embryol Morphogen* 6:335–346.
- Reckova M, Rosengarten C, deAlmeida A, Stanley CP, Wessels A, Gourdie RG, Thompson RP, Sedmera D. 2003. Hemodynamics is a key epigenetic factor in development of the cardiac conduction system. *Circ Res* 93:77–85.
- Rentschler S, Harris BS, Kuznekoff L, Jain R, Manderfield L, Lu MM, Morley GE, Patel VV, Epstein JA. 2011. Notch signaling regulates murine atrioventricular conduction and the formation of accessory pathways. *J Clin Invest* 121:525–533.
- Sankova B, Benes J Jr, Krejci E, Dupays L, Theveniau-Ruissy M, Miquerol L, Sedmera D. 2012. The effect of connexin40 deficiency on ventricular conduction system function during development. *Cardiovasc Res* 95:469–479.
- Sankova B, Machalek J, Sedmera D. 2010. Effects of mechanical loading on early conduction system differentiation in the chick. *Am J Physiol Heart Circ Physiol* 298:H1571–H1576.
- Schaefer KS, Doughman YQ, Fisher SA, Watanabe M. 2004. Dynamic patterns of apoptosis in the developing chicken heart. *Dev Dyn* 229:489–499.
- Sedmera D, Harris BS, Grant E, Zhang N, Jourdan J, Kurkova D, Gourdie RG. 2008. Cardiac expression patterns of endothelin-converting enzyme (ECE): implications for conduction system development. *Dev Dyn* 237:1746–1753.
- Sedmera D, Kockova R, Vostarek F, Raddatz E. 2015. Arrhythmias in the developing heart. *Acta Physiol (Oxf)* 213:303–320.
- Sugishita Y, Leifer DW, Agani F, Watanabe M, Fisher SA. 2004. Hypoxia-responsive signaling regulates the apoptosis-dependent remodeling of the embryonic avian cardiac outflow tract. *Dev Biol* 273:285–296.
- Vicente-Steijn R, Kolditz DP, Mahtab EA, Askar SF, Bax NA, Van Der Graaf LM, Wisse LJ, Passier R, Pijnappels DA, Schaliij MJ, Poelmann RE, Gittenberger DEGAC, Jongbloed MR. 2010. Electrical activation of sinus venosus myocardium and expression patterns of RhoA and *Isl-1* in the chick embryo. *J Cardiovasc Electrophysiol* 21:1284–1292.
- Vicente-Steijn R, Passier R, Wisse LJ, Schaliij MJ, Poelmann RE, Gittenberger-de Groot AC, Jongbloed MR. 2011. Funny current channel HCN4 delineates the developing cardiac conduction system in chicken heart. *Heart Rhythm* 8:1254–1263.
- Watanabe M, Jafri A, Fisher SA. 2001. Apoptosis is required for the proper formation of the ventriculo-arterial connections. *Dev Biol* 240:274–288.
- Wessels A, Vermeulen JL, Viragh S, Kalman F, Lamers WH, Moorman AF. 1991. Spatial distribution of "tissue-specific" antigens in the developing human heart and skeletal muscle. II. An immunohistochemical analysis of myosin heavy chain isoform expression patterns in the embryonic heart. *Anat Rec* 229:355–368.
- Zhou B, von Gise A, Ma Q, Hu YW, Pu WT. 2010. Genetic fate mapping demonstrates contribution of epicardium-derived cells to the annulus fibrosis of the mammalian heart. *Dev Biol* 338:251–261.